Polymer 50 (2009) 3240–3244

Contents lists available at ScienceDirect

Polymer

journal homepage: www.elsevier.com/locate/polymer

Silicon-containing polymer nanosheets for oxygen plasma resist application

Sabiha Sultana [a], Jun Matsui [a,b,*], Seiki Mitani [a], Masaya Mitsuishi [a], Tokuji Miyashita [a,**]

[a] Institute of Multidisciplinary Research for Advanced Materials (IMRAM), Tohoku University, Katahira 2-1-1, Aoba-ku, Sendai 980-8577, Japan
[b] Precursory Research for Embryonic Science and Technology (PRESTO), Japan Science and Technology Agency, 4-1-8, Honcho, Kawaguchi 332-001, Japan

ARTICLE INFO

Article history:
Received 15 January 2009
Received in revised form
9 April 2009
Accepted 1 May 2009
Available online 12 May 2009

Keywords:
Ultrathin polymer photoresist
Langmuir–Blodgett film
Silicon-containing polymer

ABSTRACT

In this paper, we prepared a silicon-containing polymer nanosheet, poly(neo-pentylmethacrylamide-*co*-4-(trimethylsilyl)phenyl)methacrylamide (p(nPMA/SiPhMA)), for positive-tone photoresist application. p(nPMA/SiPhMA) forms a stable monolayer at the air–water interface and the polymer monolayer can be transferred onto a solid substrate using the Langmuir–Blodgett technique, when the SiPhMA molar contents are below 38%. Sixty layers of p(nPMA/SiPhMA) nanosheet were deposited onto a silicon substrate and deep UV was irradiated through a photomask to the deposited film. After development of the irradiated film with alkaline solution, a positive-tone fine pattern with a 0.75 μm resolution, which is the highest resolution of the photomask, was clearly drawn. UV–vis and FT-IR spectroscopy indicates the formation of alkaline soluble groups, such as C═O and Si–O–Si after photodecomposition. Moreover, p(nPMA/PhSiMA) polymer nanosheet shows three times higher oxygen etching resistance compared to poly(methylmethacrylate) (PMMA). The high plasma resistance of the polymer nanosheet film is caused by not only the presence of Si atom in the film but also a closely packed and high molecular orientated structure of the polymer nanosheets.

1. Introduction

Explosive growth in electronic devices industry has been supported by miniaturization of semiconductor devices [1]. Fabrication of high-resolution resist pattern by photolithography technique is a key technology to create such micro-nano sized silicon devices. High-resolution resist pattern can be drawn using advanced exposure processes such as liquid immersion lithography, ArF laser, phase shift mask and/or using elegant photoresist system such as chemically amplified photoresist and double-layered photoresist [1–3]. In the case of double-layered photoresist, the upper layer resist should be uniform, defect-free and ultrathin to draw a high-resolution pattern [2–4]. Langmuir–Blodgett (LB) film has a feature to form a defect-free and molecularly ordered ultrathin film with controlled thickness and orientation [5]. Therefore, several groups have applied LB film for ultrathin resist [6–14]. We have found that *N*-alkylacrylamide and *N*-alkylmethacrylamide polymers form a highly oriented polymer monolayer on the water surface. The polymers form a densely packed and stable polymer monolayer (polymer nanosheet) because of a two-dimensional hydrogen bonding network that exist between the amide groups [15,16]. Moreover, we have found that poly(neo-pentylmethacrylamide) works as a dry developable positive-tone photoresist and its copolymer with *N*-phenylmethacrylamide; poly(neo-pentylmethacrylamide-*co*-phenylmethacrylamide) works as a water developable positive-tone photoresist [17,18]. Thickness of the polymer nanosheet can be controlled from 1 nm to several hundreds of nanometer by changing the deposition number of layers with 1 nm periodicity. Therefore defect-free ultrathin polymer resist with 1 nm thickness can be prepared using the polymer nanosheet.

Etching is also an important process to create a high-resolution pattern. In the double-layered photoresist, usually oxygen plasma was used to transfer the upper layer resist pattern onto lower layer resist [3]. Therefore, upper layer resist requires high oxygen plasma etching resistance. It was reported that silicon-containing polymer shows high oxygen plasma resistance because of the formation of SiO_x groups during the oxygen etching process [19–22].

In this article, we incorporated silicon-containing molecule, *N*-(4-(trimethylsilyl)phenyl)methacrylamide as a comonomer of nPMA to produce ultrathin polymer photoresist with high oxygen plasma etching resistance (Fig. 1). The monolayer property of the polymer was studied by surface pressure–area isotherm. The monolayer was transferred onto a solid substrate using LB technique to produce a polymer nanosheet film and the positive-tone pattern was drawn onto the substrate by deep UV irradiation. The pattern formation was

* Corresponding author. Institute of Multidisciplinary Research for Advanced Materials (IMRAM), Tohoku University, Katahira 2-1-1, Aoba-ku, Sendai 980-8577, Japan. Tel./fax: +81 22 217 5639.
** Corresponding author. Tel.: +81 22 217 5637; fax: +81 22 217 5642.
E-mail addresses: jun_m@tagen.tohoku.ac.jp (J. Matsui), miya@tagen.tohoku.ac.jp (T. Miyashita).

0032-3861/$ – see front matter © 2009 Elsevier Ltd. All rights reserved.
doi:10.1016/j.polymer.2009.05.002

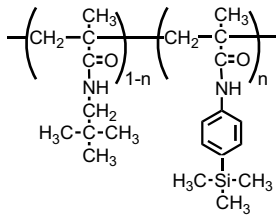

Fig. 1. Chemical structure of poly(neo-pentylmethacrylamide-*co*-(4-(trimethylsilyl)-phenyl) methacrylamide) (p(nPMA/SiPhMA)).

discussed by FT-IR and UV-vis measurements. Moreover, oxygen plasma etching property of the nanosheet film was studied.

2. Experimental

Synthesis of *N*-(4-(trimethylsilyl)phenyl)methacrylamide (SiPhMA) monomer and neo-pentylmethacrylamide (nPMA) has been described elsewhere [17,23]. Copolymers with various compositions of nPMA and SiPhMA monomer units were prepared in dried toluene at 60 °C under nitrogen by free-radical polymerization using azoisobutyronitrile (AIBN) as a thermal initiator. The polymer was purified by reprecipitation from chloroform into a large excess of hexane with three times and subsequently dried under vacuum at room temperature. The concentration of SiPhMA was determined by ^{1}H NMR spectra using peak area of CH_3 in nPMA at 0.6–1.0 ppm and CH_3 in SiPhMA at 0.1–0.4 ppm. The number average molecular weight (M_n) and polydispersity index (M_w/M_n) were determined using a gel permeation chromatograph (GPC; Tosoh Corp.) with a polystyrene standard. The number average molecular weights and polydispersities for p(nPMA/SiPhMA16), p(nPMA/SiPhMA38), and p(nPMA/SiPhMA55) are 2.50×10^4 ($M_w/M_n = 2.06$), 2.50×10^4 (2.04), and 1.70×10^4 (2.04) respectively. The UV absorption measurements were carried out using a UV-vis spectrophotometer (U-3000; Hitachi Ltd.).

A thin film of PMMA on a silicon substrate was prepared using a spin coater (Mikasa Spin Coater 1H-D7; Mikasa Co. Ltd.) from a solution of PMMA in toluene (10 wt%) at 2000 rpm for 30 s and the obtained film was baked at 110 °C for 1 min in order to evaporate the solvent. The thickness of the PMMA film was measured by a surface profiler (Dektak^{3}ST; ULVAC).

Surface pressure (π)–area (A) isotherm measurements and the deposition of p(nPMA/SiPhMA)s monolayer were carried out with computer-controlled Langmuir trough (FSD-50 and 51; USI). Distilled and deionized water (>17.5 MΩ cm, CPW-101; Advantec) was used as the subphase. The polymer monolayer was compressed at a rate of 15.0 cm^2/min. The polymer monolayer was transferred onto solid substrates using a vertical deposition method at a dipping speed of 10 mm/min under surface pressure of 18 mN/m at 15 °C. The quartz and silicon substrates on which the monolayer was deposited were cleaned by treatment with a UV–O_3 cleaner (NL-UV253; Nippon Laser and Electronics Laboratory) and were made hydrophobic by immersion of the substrates into a ca. 1×10^{-6} M octadecyltrichlorosilane (Shinetsu Chemical Co.) chloroform solution. The oxygen plasma etching was performed at 1 Pa with 20 V (L-451D; Anelva). The oxygen flow rate was 100 sccm. The FT-IR spectra were measured using a spectrometer (FTIR-230; Jasco Inc.). CaF_2 was used as a substrate for FT-IR measurements. The CaF_2 substrate was washed with acetone and chloroform before use. Deep UV irradiation was carried out with deep UV lamp (SX-UID 501MUV2QQ; USHIO) using water filter [24]. The intensity at 254 nm was 100 mW/cm^2. XPS experiments were performed using a spectrometer (PHI 5600; Perkin–Elmer Inc.) The take-off angle was fixed at 45°. All binding energies in XPS measurements were referenced to the C 1s peak for neutral carbon, which was assigned a value of 285.0 eV. The thickness of the polymer nanosheet film was measured using atomic force microscopy (SPA-400 SII; NanoTechnology Inc.). The silicon cantilever with spring constant $k = 12$ N/m (SI-DF 20; Olympus Corp.) with small tip curvature of less than 10 nm was used in non-contact mode.

3. Results and discussion

3.1. Monolayer behavior of the polymer on the water surface

p(nPMA/SiPhMA)s were spread on a water subphase from a chloroform solution (ca.1 mM) to measure the π–A isotherm at 15 °C. The isotherms show a steep rise in surface pressure and a relatively high collapse pressure, which indicate that the polymers show a stable and highly oriented monolayer at the air–water interface (Fig. 2). The isotherms are shifted toward a region of smaller surface area with increasing mole fraction of SiPhMA units. The average molecular occupied surface area per repeat unit is estimated by extrapolating the steep rising part of the π–A to zero surface pressure. The surface area for the copolymers was obtained to be 0.31, 0.30, and 0.29 nm^2/repeat unit for p(nPMA/SiPhMA16), p(nPMA/SiPhMA38), and p(nPMA/SiPhMA55), respectively. The plots of the surface area against the mole fraction of SiPhMA give a good linearity (Fig. 3), which indicates that the average surface area of the monolayers is determined by an additional rule in the surface area of SiPhMA and nPMA monomer, that is, the monomer units behave as an ideal mixing of the copolymer monolayers. The collapse pressures for the copolymer monolayers also decrease with the mole fraction of SiPhMA, which is consistent with an ideal mixing behavior. From the linear relationship in Fig. 3, the surface area of SiPhMA molecules is estimated to be approximately 0.27 nm^2/monomer unit. The theoretical surface areas of SiPhMA were calculated based on the Corey–Pauling–Koltun (CPK) model (inset in Fig. 4). A comparison of the surface area value derived from the π–A isotherm with calculated results suggests that SiPhMA takes perpendicular orientation on the air–water interface as shown in Fig. 4. The molecular length of SiPhMA is longer than nPMA, therefore trimethylsilyl groups of SiPhMA were overlapped with neo-pentyl groups of nPMA, which results in a smaller surface

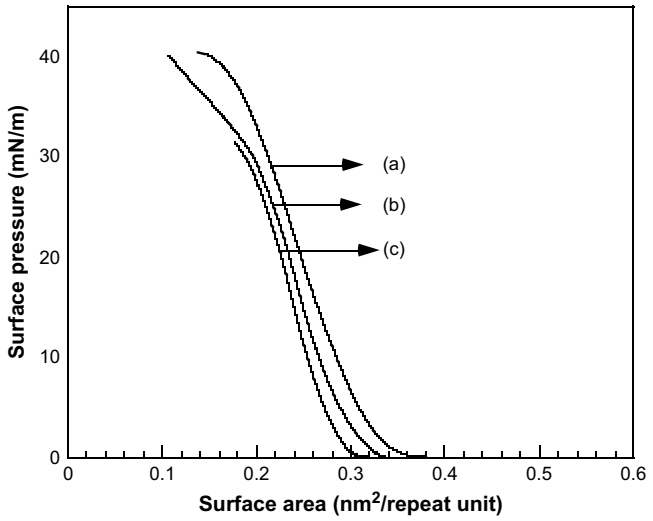

Fig. 2. Surface pressure (π)–area (A) isotherms of p(nPMA/SiPhMA) nanosheets at the air–water interface measured at 15 °C. (a) p(nPMA/SiPhMA16), (b) p(nPMA/SiPhMA38), and (c) p(nPMA/SiPhMA55).

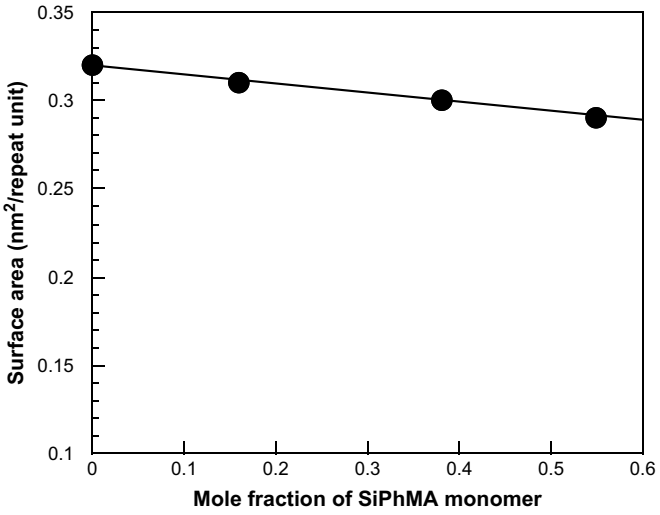

Fig. 3. Molecular occupied surface area as a function of mole fraction of SiPhMA.

area of the measured value (0.27 nm^2) than that of the theoretical value assuming a perpendicular orientation (0.33 nm^2).

Higher concentration of silicon atom is required for achieving high oxygen plasma resistance in a polymer photoresist. On the other hand, the collapse pressure of the copolymer decreases with increasing SiPhMA, which indicates that the copolymer monolayer becomes unstable with increasing the SiPhMA content. This can be explained by the fact that SiPhMA monomer has a low ability to form a stable monolayer, whereas nPMA has an excellent ability to form a stable monolayer. Indeed, p(nPMA/SiPhMA55) polymer monolayer is difficult to transfer onto a substrate. Therefore, p(nPMA/SiPhMA38) was chosen for the further experiment. UV absorption spectra of p(nPMA/SiPhMA38) deposited film onto quartz substrate were measured as a function of the number of deposited layers. The absorbance at around 254 nm which is assigned to the absorption of phenyl group of SiPhMA, increased linearly with increasing deposition number of layers. The linear relationship between the absorbance and the number of layers suggests that a regular deposition of the monolayer takes place resulting in a fairly uniform nanosheet film (Fig. 5).

3.2. Drawing fine positive patterns on the polymer nanosheets

To draw a positive pattern, p(nPMA/SiPhMA38) polymer nanosheet film with 60 layers was exposed to a deep UV lamp through

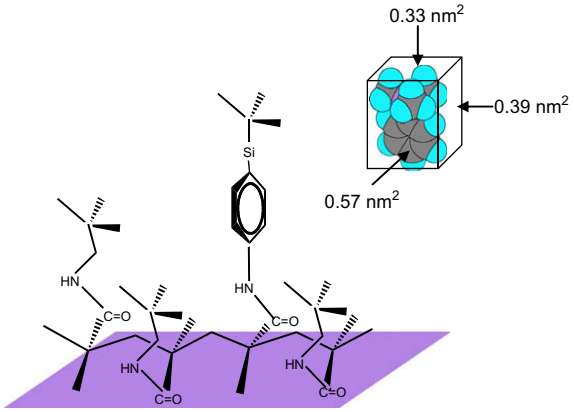

Fig. 4. Proposed orientation of p(nPMA/SiPhMA) monolayer at the air–water interface. Inset: calculated areas of cross-section of SiPhMA using CPK model.

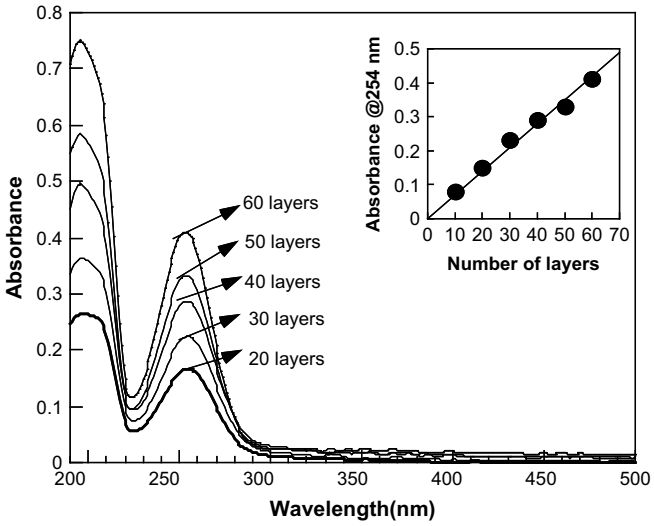

Fig. 5. Absorption spectra of p(nPMA/SiPhMA38) nanosheet as a function of deposited number of layers. Inset: a linear relationship between the absorbance and the number of layers.

a photomask in air for 35 min. Development of the nanosheet film was carried out with 0.3% tetramethylammonium hydroxide (TMAH) aqueous solution. The optical microscope image indicates that the fine patterns based on the line-and-space with a resolution of 0.75 μm, which is the highest resolution of the photomask employed in this study, can be clearly drawn with no swelling (Fig. 6). It should be mentioned that the high resolution is achieved in a simple contact printing. These findings suggest that the photodecomposition of p(nPMA/SiPhMA38) takes place under deep UV irradiation, resulting in the formation of alkali-developable fragments as shown in the following section.

The film thickness of the exposed portion as a function of exposure time was measured to estimate the contrast of the positive resist. The normalized nanosheet film thickness was determined from the ratio of the nanosheet film thickness after development for each given exposure time to the nanosheet thickness prior to the exposure. Obviously, the normalized nanosheet thickness decreases with increasing exposure time; the polymer was decomposed effectively and became alkali-developable by the deep UV irradiation on the nanosheet film. From the shape of the plot, the contrast

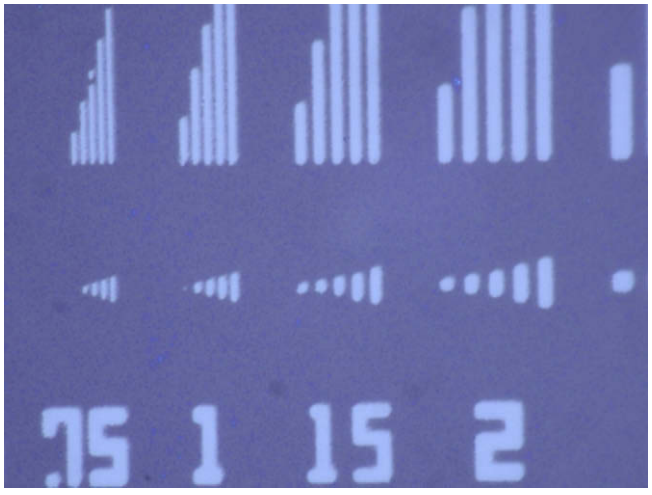

Fig. 6. Optical micrograph of positive-tone fine patterns of p(nPMA/SiPhMA38) nanosheet with 60 layers on a silicon wafer after deep UV irradiation followed by development with 0.3% TMAH aqueous solution.

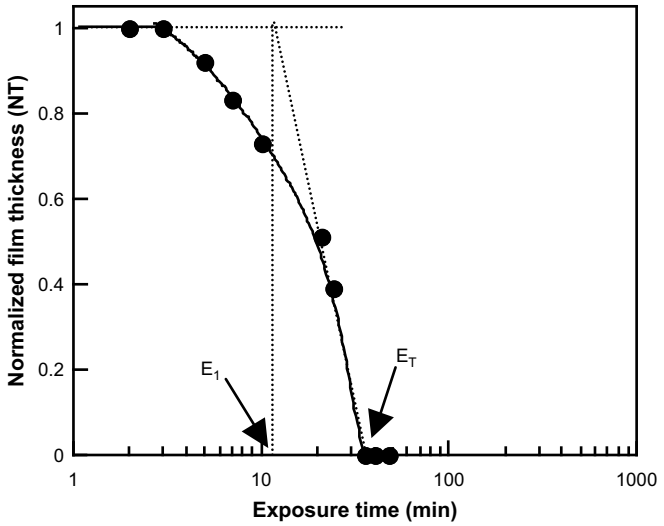

Fig. 7. Decrease in film thickness of p(nPMA/SiPhMA38) nanosheet with deep UV irradiation. 60 layers (61 nm) of p(nPMA/SiPhMA38) were deposited onto a substrate to obtain the curve.

(γ) of the polymer nanosheet film was obtained to be 3.4 (Fig. 7). The contrast was calculated using the equation, $\gamma = 1/\log(E_T/E_1)$ where E_T is the threshold energy where the irradiated area was completely soluble to the developer and E_1 is the energy obtained by extrapolating the linear potion of sensitivity curve to NT = 1. The sensitivity (>200 J/cm^2) of the p(nPMA/SiPhMA) polymer nanosheet resist is too low for industrial application. We have reported that polymer nanosheet containing *tert*-butoxycarbonyl (*t*Boc) group, poly(*N*-dodecylacrylamide-*co*-*tert*-butyl 4-vinylphenyl carbonate) (p(DDA/*t*BVPC)), works as a chemically amplified photoresist. Therefore, the sensitivity will be increased by using tri-copolymer nanosheet of p(nPMA/SiPhMA/*t*BVPC) or hetero-deposited film of p(nPMA/SiPhMA) and p(DDA/*t*BVPC) as a resist [25,26].

3.3. Photopatterning mechanism of polymer nanosheet film

Photopatterning mechanism was discussed by UV–vis and FT-IR absorption spectra measurements. UV–vis absorption spectral

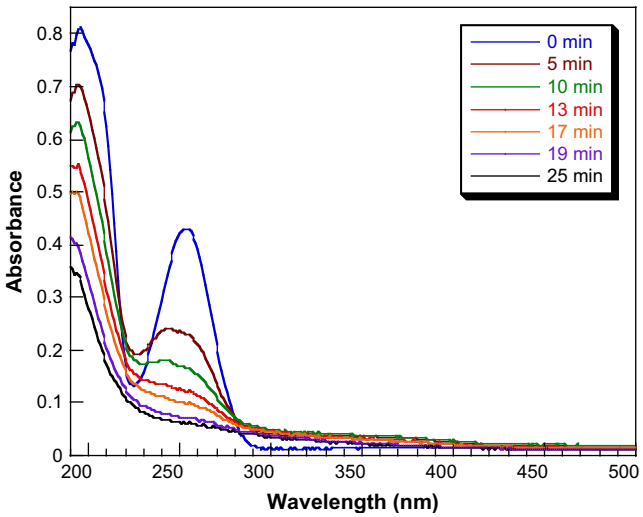

Fig. 8. Change in UV absorption spectra of p(nPMA/SiPhMA38) nanosheets with the function of deep UV irradiation time.

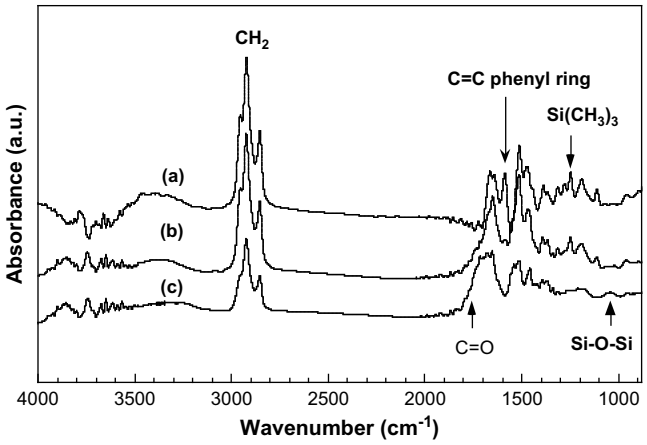

Fig. 9. FT-IR spectra of 100 layers of p(nPMA/SiPhMA38) nanosheets with different deep UV irradiation time: (a) 0 min, (b) 10 min and (c) 35 min.

change of p(nPMA/SiPhMA38) polymer nanosheet film with 60 layers under deep UV irradiation was measured (Fig. 8). The absorption band at around 254 nm which is attributed to the π–π^* transition of phenyl group of SiPhMA and the band at around 200 nm assigned to carbonyl group of nPMA and SiPhMA were decreased with irradiation time. The decrease in 254 nm is faster than 200 nm, which indicates that SiPhMA decomposition is predominant. FT-IR spectra of nanosheet film with 100 layers before [Fig. 9 (a)] and after [Fig. 9(b) and (c)] deep UV irradiation show similar results. After photoirradiation, the IR absorption band of phenyl ring (1594 cm^{-1}) and Si–CH$_3$ stretching (1247 cm^{-1}) was rapidly decreased and became negligible after 35 min. On the other hand, two new bands were formed at around 1050 cm^{-1} and 1720 cm^{-1}, which are assigned to Si–O–Si stretching of SiO$_x$ and C═O of ketone, aldehyde, or carboxylic acid. The formation of SiO$_x$ group was also confirmed by Si 2p XPS spectrum (Fig. S1 in Supplementary data). The spectroscopic results indicate that SiPhMA of p(*n*PMA/SiPhMA) was photooxidized to form SiO$_x$ and C═O group by deep UV irradiation. From the previous results, direct decomposition of neo-pentylacrylamide groups is negligible in this energy dose [17,18,27].

3.4. Oxygen plasma etching property of p(nPMA/SiPhMA38) polymer nanosheet film

Etching resistance of the p(nPMA/SiPhMA38) nanosheet film toward oxygen plasma was compared with a conventional polymer, poly(methylmethacrylate) (PMMA) spin-coated film and p(nPMA/SiPhMA38) spin-coated film. p(nPMA/SiPhMA38) nanosheet film with 100 layers deposited on a silicon substrate, PMMA spin-coated film, and p(nPMA/SiPhMA38) spin-coated film on a silicon wafer were put into a chamber and oxygen plasma etching (5 min) was carried out. The thickness of 100 layers of p(nPMA/SiPhMA38) is measured to be 104 nm (rms = 2.4 nm) (Fig S2 in Supplementary data), which indicates that the monolayer thickness of p(nPMA/SiPhMA38) is 1 nm. This value is consistent with the monolayer thickness of nPMA homopolymer nanosheet film [18], which supports the uniform deposition of p(nPMA/SiPhMA38) nanosheet film. After oxygen plasma etching, the decrease in film thickness was observed for the three samples. The average etching rate of the film was determined to be 42 nm/min for PMMA spin-coated film, 21 nm/min for p(nPMA/SiPhMA38) spin-coated film, and 16 nm/min for p(nPMA/SiPhMA38) nanosheet film. p(nPMA/SiPhMA38) polymer shows higher etching resistance in an oxygen plasma than

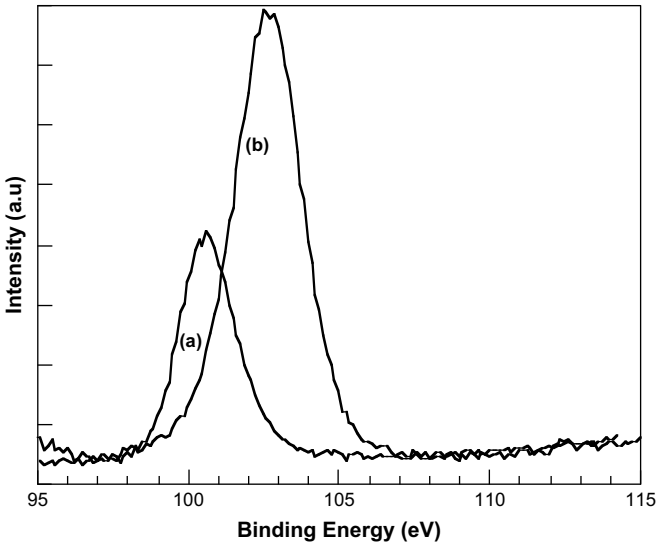

Fig. 10. Si 2p core-level XPS spectra of p(nPMA/SiPhMA38) nanosheets of 100 layers before (a) and after (b) oxygen plasma etching.

PMMA. XPS measurement was carried out to determine the chemical composition of p(nPMA/PhSiMA38) nanosheet film (Fig. 10). The core-level XPS spectrum of Si in p(nPMA/PhSiMA38) film shows a binding energy centered at 100.5 eV before oxygen plasma etching. This peak is attributed to Si–C bonding. After carrying out oxygen plasma etching, the peak was shifted to 102.5 eV, which is attributed to Si–O_x [28]. The XPS results indicate that silicon atom in the polymer was converted to silicon oxide during oxygen plasma etching, which increases the oxygen plasma etching resistance. The presence of a protective silicon oxide layer reduces the etching rate of silicon-containing polymer nanosheet film and hardens the surface. Moreover, p(nPMA/SiPhMA38) nanosheet film shows 1.3 times higher etching resistance than its spin-coated film, which indicates that the closely packed and high molecular oriented structure of polymer nanosheets also increases the etching resistance. Eventually, p(nPMA/SiPhMA38) nanosheet film shows 2.6 times higher etching resistance than PMMA. Moreover, we carried out short oxygen plasma etching (30 s) for p(nPMA/SiPhMA) polymer nanosheet and PMMA spin coating film. The etching rate was 8 nm/min for p(nPMA/SiPhMA) polymer nanosheet and 16 nm/min for PMMA film. The extremely short etching time results in low etching rate, however, the etching resistance of p(nPMA/SiPhMA) polymer nanosheet is still higher than that of PMMA spin-coated film.

4. Conclusion

Silicon-containing polymer p(nPMA/SiPhMA) nanosheet films were prepared and applied to a positive-tone photoresist. Deep UV irradiation on the copolymer nanosheet film produced a positive-tone fine pattern with a 0.75 μm resolution after developing with alkaline solution. Spectroscopic measurements reveal that C═O and Si–O groups, which increase solubility against alkaline solution were formed after photoirradiation. Moreover, the polymer nanosheet film shows three times higher oxygen plasma etching resistance compared to that of PMMA. The high oxygen plasma resistance and the ability to form a closed packed ultrathin film of p(nPMA/SiPhMA) support its application to upper resist in double-layered photoresist.

Acknowledgments

The authors would like to thank Prof. Kaino, Prof. Sugihara and Dr. Cai for oxygen plasma etching experiment. This research was partially supported by Grant-in-Aid for Science Research (No. 17105006) from the Ministry of Education, Culture, Sports, Science and Technology of Japan. J.M. acknowledges financial support from the Asahi Glass Foundation. S.S. acknowledges financial support from Japanese Government for *Monbukagakusho* Scholarship Program for International Students.

Appendix. Supplementary data

Supplementary data associated with this article can be found in the online version, at doi:10.1016/j.polymer.2009.05.002.

References

[1] Sze MS. Semiconductor devices physics and technology. 2nd ed. Taiwan: John Wiley & Sons; 2001.
[2] Peters R, Cobb J, Parker C. J Photopolym Sci Technol 2004;17(3):465–73.
[3] Mack C. Fundamental principles of optical lithography. Chichester: John Wiley & Sons Ltd; 2007.
[4] Bowden M, Malik S, Dilocker S. J Photopolym Sci Technol 2003;16(4):629–35.
[5] Ulman A. An introduction to ultrathin organic films from Langmuir–Blodgett to self assembly. San Diego: Academic Press; 1991.
[6] Kuan SWJ, Frank CW, Fu CC, Allee DR, Maccagno P, Pease RFW. J Vac Sci Technol B 1988;6(6):2274–9.
[7] Barraud A, Rosilio C, Ruaudelteixier A. Thin Solid Films 1980;68(1):91–8.
[8] Mathauer K, Schmidt A, Knoll W, Wegner G. Macromolecules 1995;28(4):1214–20.
[9] Matveeva NK, Bokov YS. Thin Solid Films 1992;210(1–2):477–9.
[10] Yoshimura T, Asai N, Shiraishi H, Okazaki S. Jpn J Appl Phys Part 2 1994;33(7A):L970–2.
[11] Ogawa S, Phatak JG, Morita S. J Photopolym Sci Technol 1998;11:585–8.
[12] Li XD, Aoki A, Miyashita T. Macromolecules 1997;30(7):2194–6.
[13] Aoki A, Nakaya M, Miyashita T. Macromolecules 1998;31(21):7321–7.
[14] Barraud A. Thin Solid Films 1983;99(1–3):317–21.
[15] Mitsuishi M, Matsui J, Miyashita T. Polym J (Tokyo) 2006;38(9):877–96.
[16] Matsui J, Sato Y, Mikayama T, Miyashita T. Langmuir 2007;23(16):8602–6.
[17] Guo YZ, Feng F, Miyashita T. Bull Chem Soc Jpn 1999;72(10):2149–53.
[18] Guo YZ, Mitsuishi M, Miyashita T. Macromolecules 2001;34(11):3548–51.
[19] Chan VZH, Thomas EL, Frommer J, Sampson D, Campbell R, Miller D, et al. Chem Mater 1998;10(12):3895–901.
[20] Macdonald SA, Schlosser H, Clecak NJ, Willson CG, Frechet JMJ. Chem Mater 1992;4(6):1364–8.
[21] Hartney MA, Hess DW, Soane DS. J Vac Sci Technol B 1989;7(1):1–13.
[22] Ohnishi Y, Suzuki M, Saigo K, Saotome Y, Gokan H. Proc Soc Photo-Opt Instrum Eng 1985;539:62–9.
[23] Sadighi JP, Singer RA, Buchwald SL. J Am Chem Soc 1998;120(20):4960–76.
[24] Spectrum of the deep UV lamp can be found in following website, http://www.ushio.com.cn/_file/ProductFile/File_136.pdf.
[25] Li TS, Mitsuishi M, Miyashita T. Thin Solid Films 2001;389(1–2):267–71.
[26] Li TS, Mitsuishi M, Miyashita T. Thin Solid Films 2008;516(8):2115–9.
[27] Sultana S, Matsui J, Mitsuishi M, Miyashita T. Polym J (Tokyo) 2008;40(10):953–7.
[28] Barr TL. Modern ESCA. The principles and practice of X-ray photoelectron spectroscopy. Florida: CRS Press; 1994.